ISSN No: -2456-2165 https://doi.org/10.38124/ijisrt/26jan986

Mathematical Modelling and Optimization of Soil Settlement at Bridge Approach Slabs in Kaduna State, Nigeria

Asma'u Kankia Hamdana[1*]; Abdulfatai Adinoyi Murana[2]; Jibrin Mohammed Kaura[3]; Joshua Ochepo[4]

[1,2,3,4]Department of Civil Engineering, Ahmadu Bello University, Zaria, Kaduna State, Nigeria

Corresponding Author: Asma'u Kankia Hamdana[1*]

Publication Date: 2026/02/20

Abstract: Soil settlement at bridge approach slab causes ride discomfort, cracks, and uneven surface that can cause accidents, and reduces the functionality of a bridge. Therefore, the mathematical modeling and optimization of soil settlement at bridge approach slabs was conducted in Kaduna State, Nigeria. Soil samples were collected from five (5) study locations, three of which were from a bridge settlement site in Kaduna Metropolis, and two (2) from Zaria, Kaduna state. The soil samples were tested and Plasticity Index (PI), soaked California Bearing Ratio (CBR), Unconfined Compressive Strength (UCS), cohesion, internal friction angle, and total settlement of the soil samples were obtained. Design Expert v13 (2021) software was used for the mathematical modeling and optimization. Results from the findings showed that the fifth order model significantly predicts soil settlement with R^2-values, actual-predicted R^2-values all greater than 0.9(90% accuracy). Also, the incorporation of CKD significant improves the geotechnical properties of the soil, and the optimization result showed that CKD content of 9-10% is the optimum dosage required for soil improvement. Validation of the optimized result has Absolute Percentage Error (APE) between the experimental and optimized results ranging from 0.3-3.8%. Hence, the error is minimal, and the validated result is adequate.

Keywords: *Approach Slab; Bridge; Modelling; Optimization; Settlement; Soil.*

How to Cite: Asma'u Kankia Hamdana; Abdulfatai Adinoyi Murana; Jibrin Mohammed Kaura; Joshua Ochepo (2026) Mathematical Modelling and Optimization of Soil Settlement at Bridge Approach Slabs in Kaduna State, Nigeria. *International Journal of Innovative Science and Research Technology*, 11(1), 3637-3652. https://doi.org/10.38124/ijisrt/26jan986

I. INTRODUCTION

➢ *Background of Study*

Bridge approach slabs are crucial structural components that ensure a seamless transition between the roadway embankment and the bridge deck [1]. Their principal function is to distribute loads and reduce the difference in settling between the flexible pavement and the rigid bridge structure [2]. However, one of the most persistent issues in bridge architecture is soil settlement beneath approach slabs, which frequently results in bumps, cracks, and uneven surfaces [3, 4]. These flaws degrade ride quality, raise maintenance costs, and may endanger road users [5, 6].

Soil settlement at bridge approaches is affected by a number of factors, including soil type, compaction quality, moisture changes, traffic load, and environmental conditions [7, 8]. In many cases, the embankment soils have compressibility or insufficient bearing capacity, causing differential settlement between the bridge deck and the adjacent roadway [8]. This phenomenon, popularly referred to as the "bridge bump," has been widely observed in both industrialized and developing countries as a key cause of early deterioration of bridge structures [9].

Soil settlement concerns are common in Nigeria [10-12], notably in Kaduna State [13, 14], due to the diversity of geotechnical conditions, which range from lateritic soils to clayey deposits with varied compressibility. The mechanical behavior of underlying soils has a significant impact on the performance of bridge approach slabs [15], necessitating rigorous analysis and predictive modeling. Traditional geotechnical approaches for assessing settlement frequently rely on empirical correlations and simplistic assumptions, which may not effectively reflect the complex relationships between soil qualities, loading conditions, and environmental factors. As infrastructure needs rise, there is a greater need for more resilient and predictive techniques. Mathematical modeling and optimization offer a solid foundation for understanding and predicting soil settling features [16]. The

ISSN No: -2456-2165 https://doi.org/10.38124/ijisrt/26jan986

use of statistical and computational tools like response surface methodology (RSM) and regression analysis to create predictive models that quantify settlement behavior under various scenarios has been done by previous researchers [16-18]. Optimization techniques also enable the identification of factor combinations that reduce settling, thus enhancing the longevity and serviceability of bridge approach slabs.

Furthermore, optimization approaches are critical in determining the best factor combinations that reduce settling and improve the longevity of bridge approach slabs. Design Expert software has been shown to effectively simulate geotechnical responses, validate assumptions with diagnostic plots, and ensure predictive models meet statistical adequacy criteria (e.g., R^2, adjusted R^2, predicted R^2) [19-22]. Applying these methodologies to the study area can provide an opportunity to produce localized solutions geared to tackling soil settlement of the bridge approach slab in the region. Therefore, this study of modelling and optimization of soil settlement at bridge approach slabs is essential for advancing geotechnical and structural engineering practices, which will provide a scientific basis for improving the performance of bridge infrastructure, reducing maintenance costs, and ensuring safer and more sustainable transportation systems.

II. MATERIALS AND METHODS

➢ *Materials*

The materials used for this study are natural soil samples that were gathered in polythene bags from the case studies for laboratory examinations.

The soil samples were taken from five (5) study locations, three of which were from a bridge settlement site in Kaduna Metropolis, and two (2) from Zaria, Kaduna state. Soil samples collected in Kaduna Metropolis were labelled as KDM-A, KDM-B, and KDM-C, whereas soil samples collected in Zaria were named as KDZAR-A and KDZAR-B.

➢ *Methods*

The soil samples were tested in the lab for plasticity index, soaked California Bearing Ratio (CBR), Unconfined Compressive Strength (UCS), cohesion, internal friction angle, and total settlement of the bridge settlement in accordance with relevant codes and standards (i.e., the American Association of State Highway and Transportation Officials (AASHTO) and the American Society for Testing and Materials (ASTM).

➢ *Experimental Design*

The experiment was designed using Design Expert v13 (2021) software. The experimental design was based on a user-defined multilevel numerical and categorical experiment. This experiment investigated two category factors. The factors are CKD content and sample type. The first factor is numerical; the second factor is categorical.

➢ *Design Matrix*

The design matrix illustrated the experiment's structure, with each row reflecting a specific combination of Sample (Factor A) and CKD Level (Factor B), as well as the measured values for each response. The dataset is balanced, with a total of 72 runs spread across several factor combinations. Replicates were included, because certain combinations of samples and CKD levels have repeated measurements. The replicates helped confirm dependability and provided for an estimate of measurement error.

➢ *Modeling and Optimization*

The mathematical modeling was carried out using Design Expert v13. Equation 1 contains the model's basic equation, where the response (Y) is a dependent variable and the independent variables are β_i, βi_i, β_{ij}. Equation 1 displays the error Є.

$$Y = \beta_o + \sum_i \beta_i x_i + \sum_j \beta_{ii} x_j^2 \sum_{i,j} \sum_j \beta_{ij}\, x_i x_j + Є \quad (1)$$

- *Model Selection*

The R-square values, sometimes referred to as the multiple correlation coefficients calculated as indicated in Equation 2, served as the basis for the model selection.

$$R^2 = 1 - \left[\frac{SS_{residual}}{SS_{residual} + SS_{model}}\right] = 1 - \left[\frac{SS_{residual}}{SS_{total} - SS_{curvature} - SS_{block}}\right] \quad (2)$$

Where SS = sum of squares for the residual and model.

- *Model Diagnostic*

The adjusted and predicted R-squared values, shown in Equations 3 and 4, were used to assess the model's adequacy. The Adjusted R-squared measures the amount of variance around the mean explained by the model, after accounting for the number of terms in the model. If the new terms do not improve the model, the adjusted R-squared value decreases as the number of terms in the model increases. In contrast, Predicted R-squared reveals how much of the variation in new data may be explained by the model.

$$Adjusted\ R^2 = 1 - \frac{\left[\left(\frac{SS_{residual}}{df_{residual}}\right)\right]}{\left[\left(\frac{SS_{residual} + SS_{model}}{df_{residual} + df_{model}}\right)\right]} = 1 - \frac{\left[\left(\frac{SS_{residual}}{df_{residual}}\right)\right]}{\left[\left(\frac{SS_{total} - SS_{curvature} - SS_{block}}{df_{total} - df_{curvature} - df_{block}}\right)\right]} \quad (3)$$

$$Predicted\ R^2 = 1 - \frac{[PRESS]}{[SS_{residual} + SS_{model}]} = 1 - \frac{[PRESS]}{[SS_{total} - SS_{curvature} - SS_{block}]} \quad (4)$$

Where PRESS is the model's predicted residual sum of squares, which indicates how well a given model fits every design point. Equation 5 was used to determine the PRESS.

$$PRESS = \sum_{i=1}^{n} (e_{-i})^2 \quad (5)$$

Where e_{-i} is a deletion residual calculated by fitting a model without the i^{th} run, then predicting the i^{th} observation with the resulting model.

ISSN No: -2456-2165 https://doi.org/10.38124/ijisrt/26jan986

➢ *Model Validation*

The developed mathematical models were validated using the normal plots, and predicted versus actual plots. Equations 6 and 7 shows the equations of the various model diagnostics used to validate the model.

- *Normal Plot Versus Residuals*

The normal plot of residuals was used to determine if residuals (errors) follow a normal distribution, as many statistical models assume. Residuals are defined as;

$$e_i = y_i - \tau_i \quad (6)$$

Where = observed response for observation i

τ_i = predicted response from the regression model

- *Predicted Versus Actual Plots*

Using Equation 7, we compared the model's predicted responses to the empirically observed (actual) responses.

$$y_i = \beta_o + \sum_{j=1}^{p} \beta_j X_{ij} + \sum_{j=1}^{p} \beta_{jj} X_{ij}^2 + \sum_{j<k}^{p} \beta_{jk} X_{ij} X_{ik} \quad (7)$$

➢ *Numerical Optimization*

A hill climbing method was used in the numerical optimization. Equation 9 provides the hill climbing optimization formula.

$$f(x,y) = e^{-(x^2+y^2)} \quad (9)$$

- *Optimization Validation*

As stated in Equation 10, the difference between the optimized and laboratory validated results was measured using the absolute relative percentage error (APE).

$$\text{APE} = \left[1 - \frac{\text{Predicted}}{\text{Actual}}\right] \text{x } 100 \quad (10)$$

III. RESULTS AND DISCUSSION

➢ *Model Summary Statistics*

In Table 1, the fit statistics indicates that the parameters fit a fifth order model, and how strong the prediction models are. The R^2 for the plasticity index (PI), the soaked CBR, the unconfined compression strength (UCS), the cohesion (C), the angle of internal friction (ϕ) and the total settlement are all above 0.8 (80%) which is an indication of very strong models (see Appendix for model perfromance). Likewise, the predicted R^2 for each of the six properties are all in reasonable agreement with their corresponding adjusted R^2. That is the difference of each is less than 0.2.

Table 1 The Fit Statistics

Parameter		R^2 Values					
	Model	PI	CBR	UCS	C	ϕ	Δ
R^2	Fifth Order	0.9974	0.9983	0.9932	0.8923	0.9036	0.9948
Adjusted R^2	Fifth Order	0.9956	0.9970	0.9899	0.8787	0.8820	0.9909
Predicted R^2	Fifth Order	0.9940	0.9957	0.9867	0.8609	0.8670	0.9869

➢ *Analysis of Variance (ANOVA) of the Models*

The Analysis of Variance (ANOVA) results for each parameter with respect to the different locations where soil samples were obtained are presented. Tables 2-7 represent ANOVA of the predicted response surface models.

Table 2 ANOVA for Plasticity Index Response Surface Model

Source	Sum of Squares	df	Mean Square	F-value	p-value	
Model	1.93	29	0.0666	557.77	< 0.0001	significant
A-Sample	0.8449	5	0.1690	1414.96	< 0.0001	
B-CKD	0.2228	1	0.2228	1865.50	< 0.0001	
AB	0.3029	5	0.0606	507.23	< 0.0001	
B^2	0.2707	1	0.2707	2267.06	< 0.0001	
AB^2	0.0465	5	0.0093	77.91	< 0.0001	
B^3	0.0816	1	0.0816	683.67	< 0.0001	
AB^3	0.0273	5	0.0055	45.67	< 0.0001	
B^4	0.0149	1	0.0149	125.04	< 0.0001	
AB^4	0.1201	5	0.0240	201.07	< 0.0001	
Residual	0.3587	42	0.0001			
Lack of Fit	0.357	6	0.0008			
Pure Error	0.0000	36	0.0000			
Cor Total	1.94	71				

ISSN No: -2456-2165 https://doi.org/10.38124/ijisrt/26jan986

Table 3 ANOVA for Soaked CBR Response Surface Model

Source	Sum of Squares	df	Mean Square	F-value	p-value	
Model	1546.85	30	51.56	797.51	< 0.0001	significant
A-Sample	827.17	5	165.43	2558.77	< 0.0001	
B-CKD	620.58	1	620.58	9598.49	< 0.0001	
AB	17.34	5	3.47	53.63	< 0.0001	
B^2	28.00	1	28.00	433.08	< 0.0001	
AB^2	5.62	5	1.12	17.38	< 0.0001	
B^3	5.40	1	5.40	83.52	< 0.0001	
AB^3	21.18	5	4.24	65.51	< 0.0001	
B^4	9.33	1	9.33	144.36	< 0.0001	
AB^4	8.38	5	1.68	25.93	< 0.0001	
B^5	3.86	1	3.86	59.66	< 0.0001	
Residual	2.65	41	0.0647			
Lack of Fit	2.65	5	0.5302			
Pure Error	0.0000	36	0.0000			
Cor Total	1549.50	71				

Table 4 ANOVA for UCS Response Surface Model

Source	Sum of Squares	df	Mean Square	F-value	p-value	
Model	4.67	23	0.2030	304.85	< 0.0001	significant
A-Sample	3.26	5	0.6524	979.70	< 0.0001	
B-CKD	1.27	1	1.27	1911.49	< 0.0001	
AB	0.0456	5	0.0091	13.69	< 0.0001	
B^2	0.0223	1	0.0223	33.47	< 0.0001	
AB^2	0.0270	5	0.0054	8.10	< 0.0001	
B^4	0.0121	1	0.0121	18.24	< 0.0001	
AB^4	0.0272	5	0.0054	8.18	< 0.0001	
Residual	0.1320	48	0.0007			
Lack of Fit	0.1320	12	0.0027			
Pure Error	0.0000	36	0.0000			
Cor Total	4.70	71				

Table 5 ANOVA for Cohesion Response Surface Model

Source	Sum of Squares	df	Mean Square	F-value	p-value	
Model	1712.50	8	214.06	65.27	< 0.0001	significant
A-Sample	1338.44	5	267.69	81.62	< 0.0001	
B-CKD	347.14	1	347.14	105.85	< 0.0001	
B^2	8.40	1	8.40	2.56	0.1146	
B^3	18.52	1	18.52	5.65	0.0205	
Residual	206.61	63	3.28			
Lack of Fit	206.61	27	7.65			
Pure Error	0.0000	36	0.0000			
Cor Total	1919.11	71				

Table 6 ANOVA for Angle of Internal Friction Response Surface Model

Source	Sum of Squares	df	Mean Square	F-value	p-value	
Model	543.79	13	41.83	41.84	< 0.0001	significant
A-Sample	265.78	5	53.16	53.17	< 0.0001	
B-CKD	230.48	1	230.48	230.54	< 0.0001	
AB	30.10	5	6.02	6.02	0.0001	
B^2	8.77	1	8.77	8.77	0.0044	
B^4	8.68	1	8.68	8.68	0.0046	
Residual	57.98	58	0.9997			
Lack of Fit	57.98	22	2.64			
Pure Error	0.0000	36	0.0000			
Cor Total	601.78	71				

ISSN No: -2456-2165 https://doi.org/10.38124/ijisrt/26jan986

Table 7 ANOVA for Total Settlement Response Surface Model

Source	Sum of Squares	df	Mean Square	F-value	p-value	
Model	3.24	30	0.1080	260.01	< 0.0001	Significant
A-Sample	2.77	5	0.5535	1332.81	< 0.0001	
B-CKD	0.2655	1	0.2655	639.36	< 0.0001	
AB	0.1093	5	0.0219	52.62	< 0.0001	
B^2	0.0104	1	0.0104	25.11	< 0.0001	
AB^2	0.0217	5	0.0043	10.45	< 0.0001	
B^3	0.0173	1	0.0173	41.67	< 0.0001	
AB^3	0.0246	5	0.0049	11.87	< 0.0001	
B^4	0.0059	1	0.0059	14.25	0.0005	
AB^4	0.0148	5	0.0030	7.12	< 0.0001	
B^5	0.0023	1	0.0023	5.52	0.0236	
Residual	0.2170	41	0.0004			
Lack of Fit	0.2170	5	0.0034			
Pure Error	0.0000	36	0.0000			
Cor Total	3.26	71				

The analysis from Tables 2-7 provides sum of squares, F-value, and P-value at the 0.05 significance level. The P-values at 0.05 and 0.01 are used as a tool to evaluate the significance of each coefficient, indicating a desirable and reasonable agreement between the calculated and observed results [23], After, model reduction was applied to remove all the components that are insignificant, the ANOVA results in the tables show that all response models are statistically significant since P-values are less than 0.05 in each case. Model F-value for the plasticity index, soaked CBR, UCS, cohesion, angle of internal friction and total settlement are found as 557.77, 797.51, 304.2, 65.27, 38.49 and 41.84 respectively. The Lack of Fit (LOF) F-test was also used to check the adequacy of the model. LOF depicts the variation of the data around the fitted model [24]. From the results, the P-values of LOF for each response model are greater than 0.05, which indicates that LOF is insignificant. Therefore, the suggested models for all responses are satisfactory. The resulting model for settlement of bridge approach slabs are shown below.

- *Prediction Models for the Plasticity Index*

$$PI_{KDM-A} = 2.53 - 0.04B + 0.02B^2 - 0.004B^3 + 0.0004B^4 \quad (11)$$

$$PI_{KDM-B} = 2.37 - 0.007B + 0.004B^2 - 0.001B^3 + 0.0003B^4 \quad (12)$$

$$PI_{KDM-C} = 2.18 - 0.31B + 0.193B^2 - 0.034B^3 + 0.002B^4 \quad (13)$$

$$PI_{KDM-D} = 2.29 + 0.025B + 0.005B^2 - 0.003B^3 + 0.0004B^4 \quad (14)$$

$$PI_{KDZAR-A} = 2.39 + 0.013B + 0.010B^2 - 0.002B^3 + 0.00007B^4 \quad (15)$$

$$PI_{KDZAR-B} = 2.56 - 0.289B + 0.143B^2 - 0.025B^3 + 0.002B^4 \quad (16)$$

- *Prediction Models for the Soaked CBR*

$$CBR_{KDM-A} = 17.96 + 0.514B - 1.153B^2 + 0.458B^3 + 0.057B^4 - 0.002B^5 \quad (17)$$

$$CBR_{KDM-B} = 8.99 + 4.915B - 3.17B^2 + 0.744B^3 - 0.070B^4 + 0.002B^5 \quad (18)$$

$$CBR_{KDM-C} = 14.05 + 5.60B - 3.405B^2 + 0.773B^3 - 0.0716B^4 + 0.002B^5 \quad (19)$$

$$CBR_{KDM-D} = 16.00 + 4.23B - 2.729B^2 + 0.6823B^3 - 0.068B^4 + 0.002B^5 \quad (20)$$

$$CBR_{KDZAR-A} = 17.98 - 0.515B - 0.875B^2 + 0.439B^3 - 0.057B^4 + 0.002B^5 \quad (21)$$

$$CBR_{KDZAR-B} = 16.02 + 4.113B - 2.616B^2 + 0.633B^3 - 0.064B^4 + 0.002B^5 \quad (22)$$

- *Prediction Models for the UCS*

$$UCS_{KDM-A} = 0.592 + 0.118B - 0.061B^2 + 0.017B^3 - 0.020B^4 \quad (23)$$

$$UCS_{KDM-B} = 0.137 + 0.150B - 0.086B^2 + 0.022B^3 - 0.0022B^4 \quad (24)$$

$$UCS_{KDM-C} = 0.121 + 0.080B - 0.058B^2 + 0.018B^3 - 0.0026B^4 \quad (25)$$

$$UCS_{KDM-D} = 0.544 + 0.258B - 0.165B^2 + 0.036B^3 - 0.003B^4 \quad (26)$$

$$UCS_{KDZAR-A} = 0.259 + 0.098B - 0.059B^2 + 0.017B^3 - 0.002B^4 \quad (27)$$

$$UCS_{KDZAR-B} = 0.117 + 0.124B - 0.086B^2 + 0.022B^3 - 0.002B^4 \quad (28)$$

- *Prediction Models for the Cohesion*

$$C_{KDM-A} = 4.705 - 0.757B - 0.324B^2 - 0.019B^3 \quad (29)$$

$$C_{KDM-B} = 13.372 - 0.757B + 0.324B^2 - 0.019B^3 \quad (30)$$

$$C_{KDM-C} = 13.372 - 0.757B + 0.324B^2 - 0.019B^3 \quad (31)$$

$$C_{KDM-D} = 3.538 - 0.757B + 0.324B^2 - 0.019B^3 \quad (32)$$

$$C_{KDZAR-A} = 4.372 - 0.757B + 0.324B^2 - 0.019B^3 \quad (33)$$

$$C_{KDZAR-B} = 5.705 - 0.757B + 0.324B^2 + 0.019B^3 \quad (34)$$

- *Prediction Models for the Angle of Internal Friction (ϕ)*

$$\Phi_{KDM-A} = 38.097 - 1.648B + 0.728B^2 - 0.120B^3 + 0.006B^4 \quad (35)$$

$$\phi_{KDM-B} = 33.335 - 1.362B + 0.728B^2 - 0.120B^3 + 0.006B^4 \quad (36)$$

$$\phi_{KDM-C} = 33.097 - 1.548B + 0.728B^2 - 0.120B^3 + 0.006B^4 \quad (37)$$

$$\phi_{KDM-D} = 38.097 - 1.805B + 0.728B^2 - 0.120B^3 + 0.006B^4 \quad (38)$$

ISSN No: -2456-2165 https://doi.org/10.38124/ijisrt/26jan986

$$\phi_{KDZAR-A} = 39.335 - 1.962B + 0.728B^2 - 0.120B^3 + 0.006B^4 \quad (39)$$

$$\phi_{KDZAR-B} = 39.05 - 1.705B + 0.728B^2 - 0.120B^3 + 0.006B^4 \quad (40)$$

- *Prediction Models for the Angle of Total Settlement (δ)*

$$\Delta_{KDM-A} = 1.0007 - 0.004B + 0.015B^2 - 0.008B^3 + 0.001B^4 - 0.00006B^5 \quad (41)$$

$$\delta_{KDM-B} = 0.901 - 0127B + 0.077B^2 - 0.018B^3 + 0.002B^4 + 0.00006B^5 \quad (42)$$

$$\delta_{KDM-C} = 1.071 - 0.111B + 0.062B^2 - 0.015B^3 + 0.002B^4 + 0.00006B^5 \quad (43)$$

$$\delta_{KDM-D} = 1.442 - 0.227B + 0.091B^2 - 0.018B^3 + 0.002B^4 + 0.00006B^5 \quad (44)$$

$$\delta_{KDZAR-A} = 1.697 - 0.348B + 0.144B^2 - 0.025B^3 + 0.002B^4 + 0.00006B^5 \quad (45)$$

$$\delta_{KDZAR-B} = 1.236 - 0.072B + 0.047B^2 - 0.013B^3 + 0.001B^4 + 0.00006B^5 \quad (46)$$

All the developed models are fifth order polynomial. For the plasticity index the significant terms of the fifth order regression model are: the sample type (A), the cement kiln dust–CKD (B), the interaction between A and B, the quadratic term of B, the interaction between A and B^2, the cubic term of B, the interaction between A and B^3, the quartic term of B and the interaction between A and B^4. The fifth term B^5 is the only insignificant term in the model.

For the soaked CBR the significant terms of the fifth order regression model are: the sample type (A), the cement kiln dust–CKD (B), the interaction between A and B, the quadratic term of B, the interaction between A and B^2, the cubic term of B, the interaction between A and B^3, the quartic term of B, the interaction between A and B^4 and the fifth term B.

For the UCS, the significant terms of the fifth order regression are: the sample type (A), the cement kiln dust–CKD (B), the interaction between A and B, the quadratic term of B, the interaction between A and B^2, the quartic term of B and the interaction between A and B^4. The insignificant terms are the cubic term of B, the interaction between A and B^3 and the fifth term B.

For the cohesion, the significant terms of the fifth regression model are: the sample type (A), the cement kiln dust–CKD (B), the quadratic and the cubic terms of B. The insignificant models are the interaction between A and B, the interaction between A and B^2, the interaction between A and B^3, the quartic term of B, the interaction between A, B^4 and the fifth term B.

For the angle of internal friction, the significant terms of the fifth order regression model are: the sample type (A), the cement kiln dust–CKD (B), the interaction between A and B, the quadratic term of B and the quartic term of B. The insignificant terms are the interaction between A and B^2, the cubic term of B, the interaction between A and B^3, the interaction between A and B^4 and the fifth term B.

For the total settlement the significant terms of the fifth order regression model are: the sample type (A), the cement kiln dust–CKD (B), the interaction between A and B, the quadratic term of B, the interaction between A and B^2, the cubic term of B, the interaction between A and B^3, the quartic term of B, the interaction between A, B^4 and the fifth term B.

➢ *Diagnostics and Model Validation*

The generated models were generated using the normal plots, Box-Cox plot, and predicted vs actual plots, as shown in Figure 1 below. The Normality Plot of Residuals evaluates whether residuals follow a normal distribution, a key assumption for ANOVA and regression validity. A close alignment of points along the diagonal line confirms that the residuals are approximately normally distributed, validating the statistical model. Also, the residuals vs. predicted values plot checks for homoscedasticity and model adequacy. A random scatter of residuals around the zero line, as observed, indicates that the model's error variance is constant and no major patterns or bias exist in predictions.

ISSN No: -2456-2165 https://doi.org/10.38124/ijisrt/26jan986

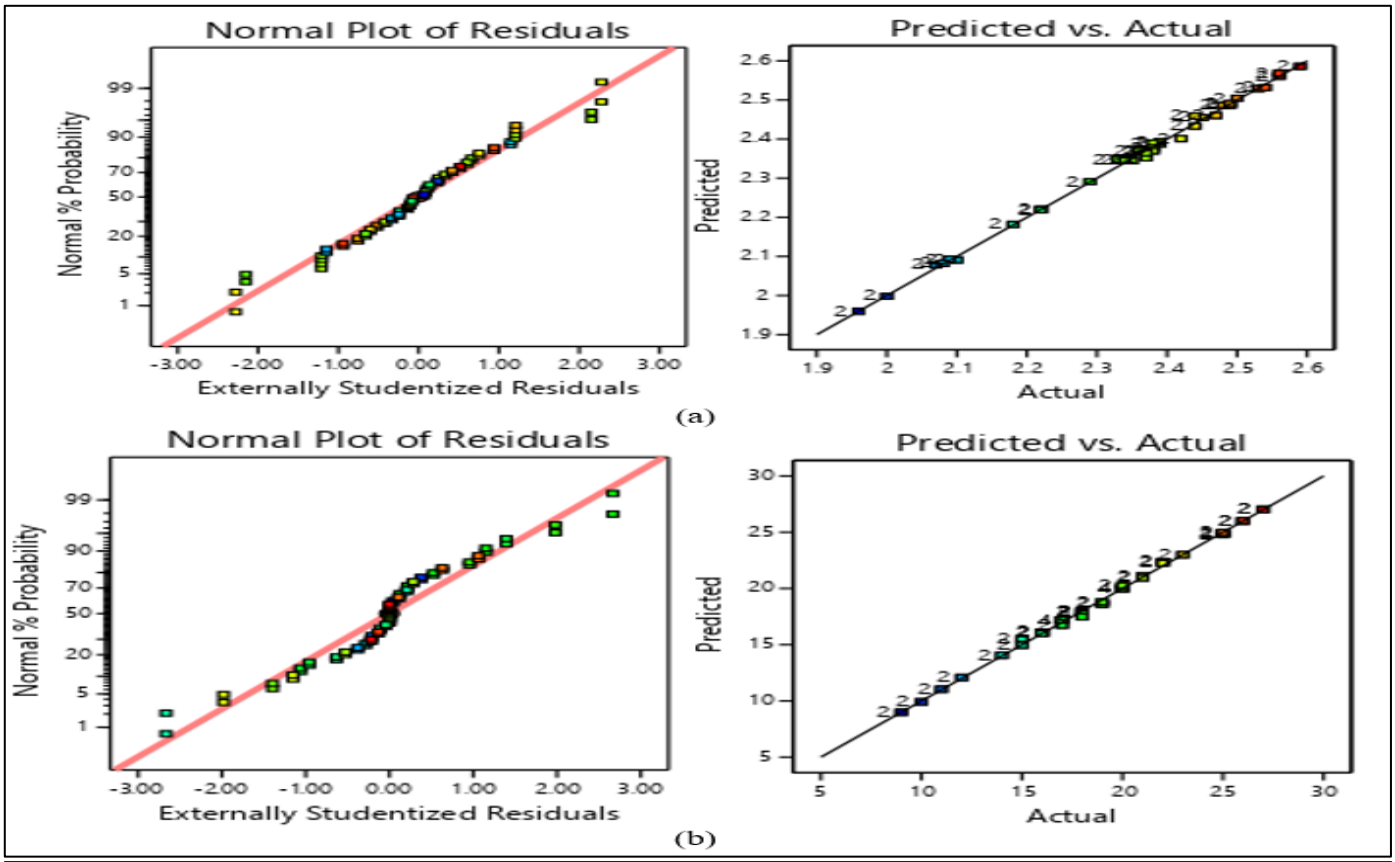

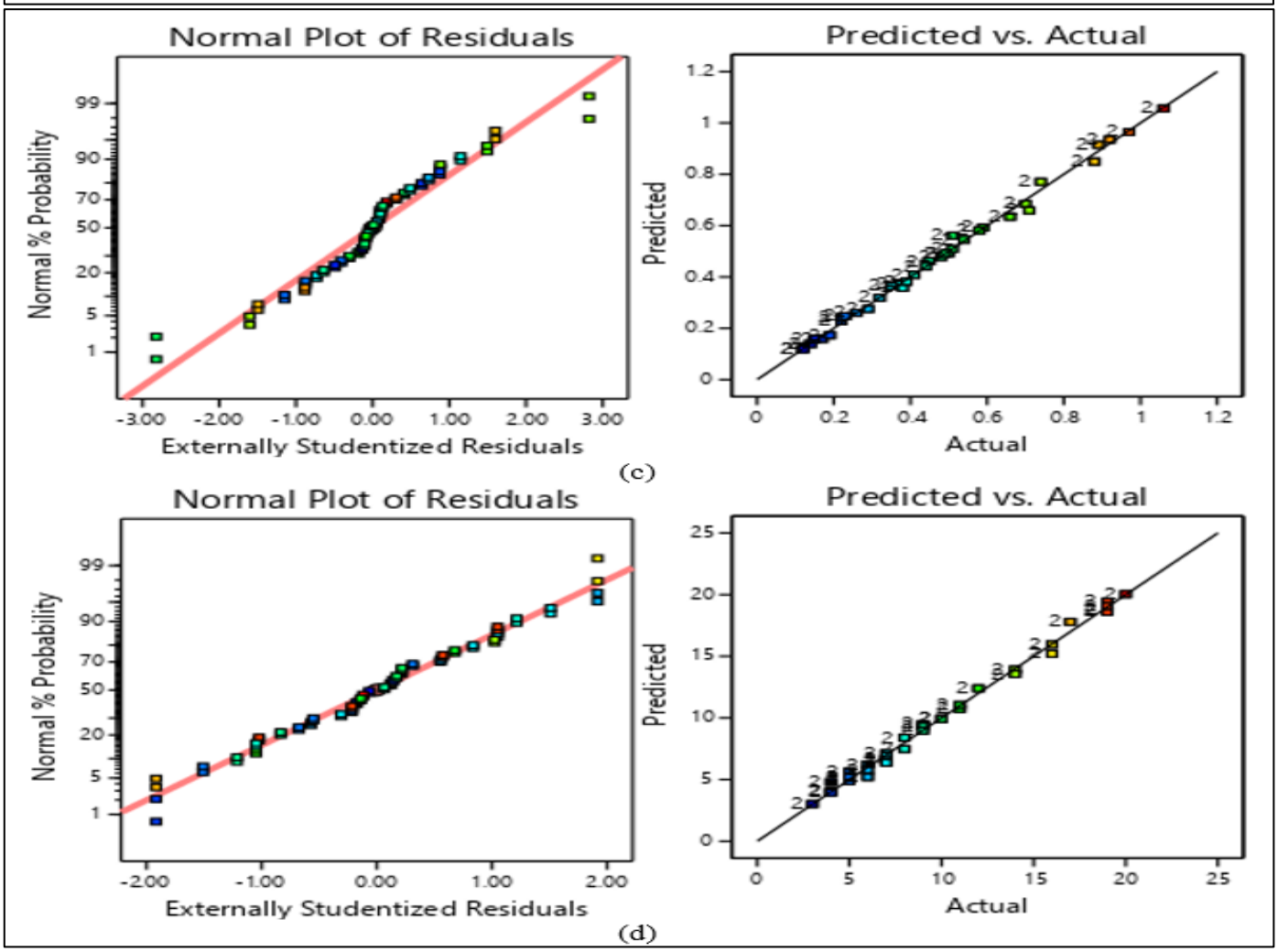

ISSN No: -2456-2165 https://doi.org/10.38124/ijisrt/26jan986

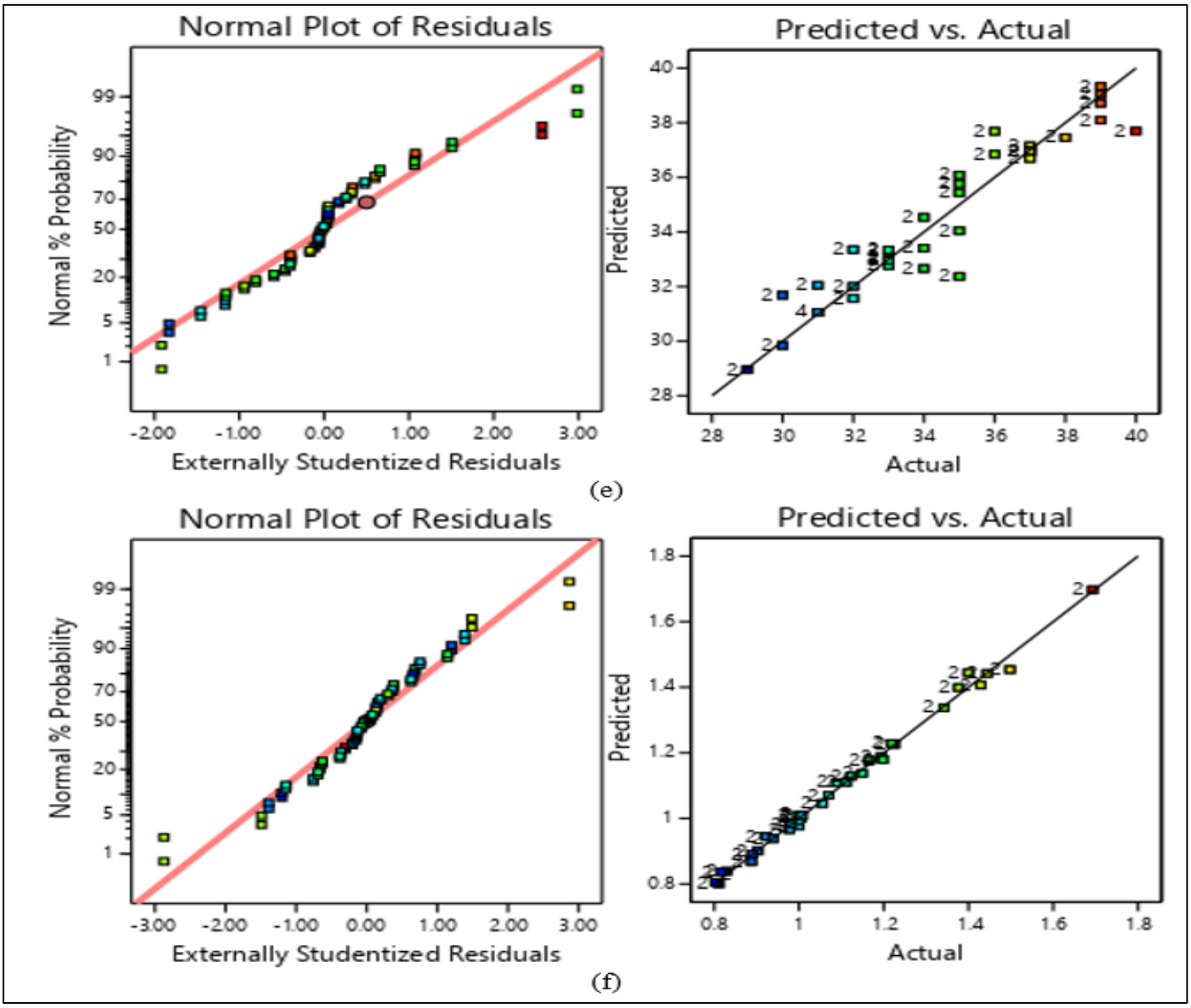

Fig 1 Normal Plots, and Plots of Predicted vs Actual for soil (a) PI; (b) CBR; (c) UCS; (d) Cohesion; (e) Internal Friction; and (f) Settlement

Figure 1(a-f) shows a linear relationship between normal plots, and predicted and actual values of the soilparameters (i.e. plasticity index, CBR, UCS, cohesion, internal friction, and settlement), indicating that the model used for prediction is accurate.Although, there is a slight discrepancy in some values, but overall, the predicted values are close to the actual measurements. However, the total Settlement plot in Fgure 1(f) shows a tighter correlation between predicted and actual values, similar to the UCS and Plasticity Index graphs.Most data points are clustered near the ideal line, suggesting that the model predicts settlement effectively.Settlement values range from 0.803 to 1.693, showing that the model can handle different settlement magnitudes with good accuracy.

➢ *Interaction Plots*

Interaction plots in this section illustrate the relationship between the dependent variable (Plasticity Index, Soaked CBR, UCS, Cohesion, Angle of Internal Friction and Total Settlement) and the two independent variables (the Sample Type and the amount of CKD), where the sample type is categorical and the CKD content is numeric. The plot helps in understanding whether the effect of the numeric variable on the response changes at different levels of the categorical variable.

The incorporation of Cement Kiln Dust into various soil types has demonstrated significant improvements in geotechnical properties, including reduced plasticity, enhanced strength parameters, and decreased settlement. These enhancements are primarily due to the pozzolanic reactions and cementitious compounds formed during the stabilization process. Therefore, CKD serves as an effective and sustainable soil stabilizer in geotechnical engineering applications [25].

ISSN No: -2456-2165 https://doi.org/10.38124/ijisrt/26jan986

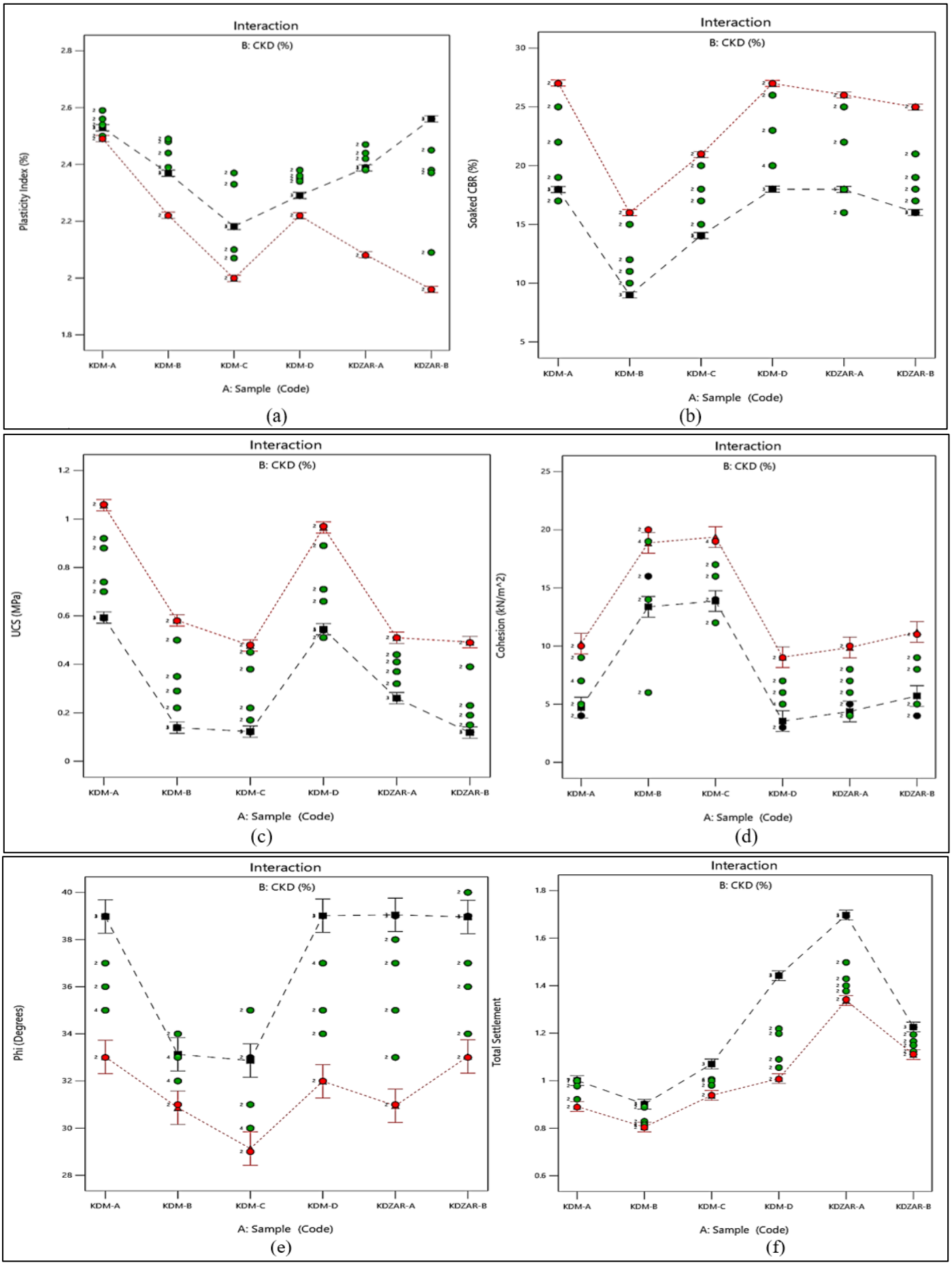

Fig 2 Interaction Plots for Soil (a) PI; (b) CBR; (c) UCS; (d) Cohesion; (e) Internal Friction; and (f) Settlement

ISSN No: -2456-2165 https://doi.org/10.38124/ijisrt/26jan986

The result from Figure 2(a) showed that the PI values for all the soil types when the CKD is 10% is the lowest. The addition of CKD to soils generally results in a reduction of the Plasticity Index, indicating decreased soil plasticity and improved workability. This reduction is attributed to the flocculation and agglomeration of clay particles facilitated by the calcium content in CKD, which diminishes the soil's plasticity [26]. Therefore, treating the soils with as much as 10% CKD is the best decision. For instance, for site KDM-B, highest PI value of 2.6 was obtained for CKD content equal to 8% and the lowest value of 2.22 was obtained from CKD content of 10%. Without addition of CKD, the PI value is 2.55. These results indicate that lowest the compressibility of the soil is achieved with the CKD content of 10%. Plasticity Index (PI) of soil is a critical parameter influencing the settlement behaviour of soils. Research indicates a strong correlation between the plasticity index and settlement characteristics of soils. Higher values of PI generally correspond to increased compressibility and settlement potential. Specifically, as the clay content increases, which raises the PI, the soil's ability to consolidate under load diminishes, leading to greater settlement over time. High plasticity soils experience rearrangement of particles under stress, further contributing to settlement.

The California Bearing Ratio (CBR) significantly impacts soil settlement as shown in Figure 2(b). Higher CBR values indicate better load-bearing capacity, reducing potential settlement under loads. Studies show that vertical confinement, such as applying surcharge rings, enhances CBR leading to improved mechanical resistance and reduced settlement. Similar trend was recorded by Gilbert [25].The relationship between CBR and soil properties, including liquid limits, underscores the importance of proper soil treatment in construction and road engineering. As shown in Figure 2, for all the six soil types (KDM-A, KDM-B, KDM-C, KDM-D, KDZAR-A and KDZAR-B), increase in the CKD content led to increased soaked CBR. This is a clear indication of the effectiveness of soil stabilisation with CKD for enhancing its load carrying capacity. Therefore, addition of the CKD will not compromise the strength of the embankment beneath the bridge approach slab.

Also, previous studies established that, unconfined compressive strength (UCS) significantly influences soil settlement, particularly in stabilized soils. Increased UCS enhances the load-bearing capacity and reduces settlement in lateritic soils treated with additives like metakaolin or zeolite. For instance, UCS can rise from 97.1 kN/m² to 2500 kN/m² with optimal additive proportions, improving durability and stability under load. Additionally, other studies shown that curing time plays a crucial role; UCS peaks at around 7 days, after which improvements are minimal. The UCS of soils improves significantly with CKD treatment. For example, the UCS of black cotton soil increased upon adding CKD . Similarly, kaolinite clay treated with 20% CKD exhibited an increase in UCS. These enhancements are attributed to the formation of calcium silicate hydrates and other cementitious compounds that bind soil particles together [26]. Thus, effective soil stabilization not only boosts UCS but also mitigates settlement issues in construction applications. CKD enhances the load-bearing capacity of soils, as evidenced by increased soaked CBR values. These improvements are due to the pozzolanic reactions between CKD and soil minerals, leading to the formation of cementitious compounds that enhance strength. Figure 4.17 displayed the effectiveness of the use of CKD in the enhancement of the soil UCS values. For all the soil type, the UCS values increases with increasing CKD content. For instance, for the soil type KDM-A, the UCS value increased from 600kN/m^2 (when the CKD value is 0) to 1050kN/m^2 (when the CKD content is 10%).

Also from Figure 2(d), the stabilisation of each of the six soil types improves the values of their cohesion except for instance for soil type KDM-B in which the addition of 2% CKD drastically reduced the cohesion from 12.5kN/m^2 (control soil) to about 6kN/m^2. CKD treatment positively influences the shear strength parameters of soils. In a study, the cohesion of treated soil increased with the addition of CKD. These improvements result from the enhanced inter-particle bonding and friction due to the cementitious products formed during the stabilization process [27]. However, for apart from this exception, the highest cohesion values are obtained at 10% CKD.

The angle of internal friction (ϕ) significantly affects soil settlement as shoen in Figure 2(e). Higher values of ϕ generally lead to increased shear strength, which can reduce settlement under load. As ϕ increases, the soil's ability to resist deformation improves, resulting in less vertical displacement when subjected to stresses. Similar trend was recorded by Eisa *et al*., (2022) In Figure 2(e), comparing with the control soil (without CKD) only sample type KDM-B, KDM-C and KDZAR-B shows increase in ϕ with increase in CKD content of 2%, 4% and 4% CKD respectively. In all other cases, the additions of CKD lead to reduction of ϕ. To address this defect, the multi-objective optimisation will generate CKD content that will lead to trade up between high cohesion and high angle of internal friction as well as favourable values of plasticity index (PI), soaked CBR, UCS as well as total settlement.

Finally from Figure 2(f), it is clear from the plot that addition of CKD drastically reduces the total settlement of the soil. For instance, for soil type KDM-D, the total settlement of the soil reduced from 1.44mm (for soil without CKD) to 0.95mm (for soil with 10% CKD stabilisation. Similar trend was recorded by Eisa *et al*., (2022).

➢ *Multi-Objective Optimization*

- *Optimization*

Multi-objective optimization process was carried out with the view to measure all six responses (plasticity index (PI), the soaked California Bearing Ratio CBR, the Unconfined Compression (UCS), Cohesion (C), Angle of Internal Friction (ϕ) and Total Settlement (δ)) simultaneously to attain a favourable CKD stabilised soil mix for all the investigated responses. Table 8 show the optimisation goals and the constraints.

ISSN No: -2456-2165 https://doi.org/10.38124/ijisrt/26jan986

Table 8 The Design Optimization Goals and the Constraints

Name	Goal	Lower Limit	Upper Limit
A: Sample	Sample Type	KDM-A	KDZAR-B
B: CKD	maximize	0	10
Plasticity Index	minimize	1.96	2.59
Soaked CBR	maximize	9	27
UCS	maximize	0.12	1.06
Cohesion	maximize	3	20
Φ	maximize	29	40
Total Settlement	minimize	0.803	1.693

The objective from Table 8, is to minimise values of plasticity index (PI) and total settlement (δ) as well as maximise values of CBR, UCS, Cohesion (C) and Angle of Internal Friction (ϕ) with maximum CKD utilization for each of the six categorical factors (sample type). The optimized result is shown in Table 9.

Table 9 Multi-Objective Optimization Solution

Sample	CKD	PI	CBR	UCS	C	ϕ	δ	Desirability
KDM-A	10.000	2.491	27.040	1.057	10.208	33.022	0.891	0.579
KDM-B	9.661	2.300	15.860	0.575	18.870	32.260	0.805	0.582
KDM-C	9.399	1.957	20.884	0.488	19.330	29.511	0.968	0.509
KDM-D	9.484	2.271	26.750	1.006	9.013	33.501	1.021	0.649
KDZAR-A	9.781	2.158	25.695	0.499	9.878	31.766	1.344	0.518
KDZAR-B	10.000	1.959	24.980	0.492	11.208	33.042	1.110	0.633

Optimization of soil stabilization parameters, including CKD content, has been validated in various studies, demonstrating its efficacy in predicting and enhancing soil mechanical properties [28]. The optimization process from Table 9 has given several solutions, but 10 %, 9.661%, 9.399%, 9.484%, 9.781% and 10% CKD content have shown the highest desirability of 0.579, 0.582, 0.509. 0.649, 0.518 and 0.633 respectively for soil category KDA-A, KDM-B, KDM-C, KDM-D, KDZAR-A and KDZAR-B.

- *Validation*

To validate the predicted mathematical models of soil properties beneath the approach slab, experiments were conducted with optimized CKD content and total settlement categorical factor. The close alignment of experimental and predicted settlement values, as observed in soil samples KDM-A through KDZAR-B, confirms the validity of the RSM models in evaluating soil behavior under optimized CKD content. This reflects the outcomes in related studies, where statistical models based on experimental design have successfully predicted mechanical soil responses [29].

The use of CKD as a stabilizing agent has been shown to enhance stiffness and reduce total settlement, especially when applied at optimal proportions. For example, Parsons and Milburn [30] demonstrated effective settlement control in subgrades using CKD, with laboratory values closely matching modeled results [30]. This is supported by Bandara, et al. [31], who emphasized the viability of CKD in mitigating excessive differential settlements beneath pavement structures.

Table 10 Validation Upon Response Surface Values

Sample Type	Experimental Values (mm)	Optimised Values (mm)	APE (%)
KDM-A	0.873	0.891	2.02
KDM-B	0.796	0.805	1.12
KDM-C	1.002	0.968	3.51
JDM-D	0.982	1.021	3.82
KDZAR-A	1.293	1.344	3.79
KDZAR-B	1.113	1.110	0.27

The result from Table 10 shows that the minor deviations between the experimental and optimized values in this study (e.g., KDM-A: 0.873 mm vs. 0.891 mm) underscore the robustness of the model calibration and the effectiveness of CKD-induced pozzolanic reactions in reducing compressibility, consistent with prior findings. The experimental and optimized values of the total settlement of the soil are presented in Table 10. Upon validation, all the experimental values of the soil properties were closely matched to the optimized values.

The Absolute Percentage Error (APE) between the experimental and optimized results ranges from approximately 0.3-3.8%, which is less than 10%, indicating that the validated model is appropriate [32, 33].

IV. CONCLUSIONS

The fifth-order polynomial regression model developed effectively captured the nonlinear interaction between CKD content and soil properties. The model accuracy exceeded

ISSN No: -2456-2165 https://doi.org/10.38124/ijisrt/26jan986

96.9%, with high predictive reliability for total settlement and plasticity index. Variability remained in Soaked CBR and cohesion, suggesting the need for further statistical refinement. The model diagnostic further supports the robustness of the model through the normal plots, and plots of action and predicted soil settlement parameters. Also, the optimization process identified ideal CKD contents for each soil category ranging from 9.399% to 10% which corresponded with highest desirability indices. Laboratory validation confirmed that these formulations offered optimal strength and minimal settlement, confirming the suitability of CKD as a soil stabilizer for approach slabs under variable subgrade conditions.

REFERENCES

[1]. B. Prakash, A. K. Tiwari, and S. R. Dash, "Bridge Approach Settlement and its Mitigation Schemes: A Review," Transportation Research Record, vol. 2678, pp. 660 - 689, 2024.

[2]. S. Azad and B. Shafei, "Performance Evaluation of Semi-Integral Abutment Bridge Ends Based on Approach Slab Details," Journal of Bridge Engineering, vol. 30, no. 3, p. 04024117, 2025.

[3]. C. Duffy, "Investigating serviceability issues related to thermal movement accommodation in bridges," Iowa State University, 2020.

[4]. A. Purwantoro, P. Pratikso, and R. Mudiyono, "Prototype Development of Bridge Approach Model with Precast Concrete-cell Box Structure to Overcome Differential Settlement," Civil Engineering and Architecture, vol. 12, no. 3A, 2024.

[5]. G. Liu, "Structural behavior of integral abutment bridge approach slabs," University of Illinois at Urbana-Champaign, 2023.

[6]. C. Jiao, J. Peng, Y. Diao, G. Zheng, and J. Han, "Centrifuge tests study on settlement and damage modes of bridge approaches using deep-seated slab," Transportation Geotechnics, vol. 49, p. 101381, 2024.

[7]. A. Bahumdain, H. Tabatabai, and H. Titi, "Analysis of soil settlement behind bridge abutments," Transportation Geotechnics, vol. 36, p. 100812, 2022.

[8]. M. W. Falah and H. Muteb, "Applying different soil stabilization mechanisms: a review," Archives of Civil Engineering, pp. 339-358-339-358, 2023.

[9]. C. Yoo, "Geosynthetics in Sustainable Transportation Infrastructure Construction," in E3S Web of Conferences, 2023, vol. 368: EDP Sciences, p. 01004.

[10]. I. P. Ukwoma, O. Igwe, and J. C. Egbueri, "Multidimensional characterization of problematic soils linked to foundation and building failures in parts of Southeast Nigeria," Modeling Earth Systems and Environment, vol. 10, no. 3, pp. 4101-4127, 2024.

[11]. M. O. Isinkaye and Y. Ajiboye, "Natural radioactivity in surface soil of urban settlements in Ekiti State, Nigeria: baseline mapping and the estimation of radiological risks," Arabian Journal of Geosciences, vol. 15, no. 6, p. 557, 2022.

[12]. K. Akinloye, F. Akinloye, O. Orimoogunje, and B. Adeleke, "Indigenous system of soil fertility management in a typical farm settlement in Osun State, Southwestern Nigeria," Journal of Geography, Environment and Earth Science International, vol. 24, no. 4, pp. 51-60, 2020.

[13]. K. H. Asma'u, A. M. Abdulfatai, and M. K. Jibrin, "Geotechnical Investigation of Soils at Settlement of Bridge Approach Slab in Kaduna State, Nigeria," Saudi J Civ Eng, vol. 9, no. 3, pp. 65-74, 2025.

[14]. K. R. Usman, I. Shuaibuc, G. Zubairud, A. Yusuf, and A. S. A. Ghafara, "Sub-Soil Geotechnical Investigation in Soft Soils for Foundation Type Selection," International Journal of Information, Engineering & Technology, p. 74, 2022.

[15]. B. Prakash, A. K. Tiwari, S. R. Dash, and S. Patra, "Structural evaluation and performance based optimization of approach slab design for mitigating bridge approach settlement through an Indian case study," in Structures, 2024, vol. 60: Elsevier, p. 105864.

[16]. H. Fattahi, H. Ghaedi, and D. Armaghani, "Improving shallow foundation settlement prediction through intelligent optimization techniques," Computer Modeling in Engineering & Sciences, vol. 143, no. 1, p. 747, 2025.

[17]. Z. Song, S. Liu, M. Jiang, and S. Yao, "Research on the Settlement Prediction Model of Foundation Pit Based on the Improved PSO-SVM Model," Scientific Programming, vol. 2022, no. 1, p. 1921378, 2022.

[18]. W. S. Loh, R. J. Chin, L. Ling, S. H. Lai, and E. Z. X. Soo, "Application of machine learning model for the prediction of settling velocity of fine sediments," Mathematics, vol. 9, no. 23, p. 3141, 2021.

[19]. H. Wu et al., "Optimization of silty soil solidification agent ratio and mechanism of strength change based on design-expert," Journal of the Chinese Institute of Engineers, vol. 47, no. 6, pp. 674-687, 2024.

[20]. Y. Berrah, S. Brahmi, N. Charef, and A. Boumezbeur, "Swelling Clay Parameters Investigation Using Design of Experiments (A Case Study)," in Engineering Geology: IntechOpen, 2021.

[21]. K. S. Salih and V. Sreedharan, "Response Surface Method for Parameter Optimization of Soils Stabilized with an Alternative Binder," Journal of Materials in Civil Engineering, vol. 37, no. 11, p. 04025400, 2025.

[22]. G. U. Alaneme et al., "Mechanical properties optimization and Simulation of soil–saw dust ash blend using extreme vertex design (EVD) method," International Journal of Pavement Research and Technology, vol. 17, no. 4, pp. 827-853, 2024.

[23]. A. Khodaii, H. Haghshenas, H. K. Tehrani, and M. Khedmati, "Application of response surface methodology to evaluate stone matrix asphalt stripping potential," KSCE Journal of Civil Engineering, vol. 17, no. 1, pp. 117-121, 2013.

[24]. A. I. Nassar, N. Thom, and T. Parry, "Optimizing the mix design of cold bitumen emulsion mixtures using response surface methodology," Construction and Building Materials, vol. 104, pp. 216-229, 2016.

[25]. A. Gilbert, "Investigating the Effectiveness of Cement Kiln Dust as an Expansive Soil Stabilizer in Road Construction," International Journal of Research and

ISSN No: -2456-2165 https://doi.org/10.38124/ijisrt/26jan986

Innovation in Social Science, vol. 9, no. 1, pp. 1401-1412, 2025.
[26]. A. Akinbuluma, "Stabilization of Lateritic Soil Sample from Ijoko with Cement Kiln Dust and Lime," Indonesian Journal Of Civil Engineering Education, vol. 9, no. 1, pp. 1-13, 2023.
[27]. M. Eisa, M. Basiouny, A. Mohamady, and M. Mira, "Improving weak subgrade soil using different additives," Materials, vol. 15, no. 13, p. 4462, 2022.
[28]. Y. T. Zewide et al., "Application of response surface methodology (RSM) for experimental optimization in biogenic silica extraction from rice husk and straw ash," Scientific Reports, vol. 15, no. 1, p. 132, 2025.
[29]. A. Almajed, D. Srirama, and A. A. B. Moghal, "Response surface method analysis of chemically stabilized fiber-reinforced soil," Materials, vol. 14, no. 6, p. 1535, 2021.
[30]. R. L. Parsons and J. P. Milburn, "Engineering behavior of stabilized soils," Transportation Research Record, vol. 1837, no. 1, pp. 20-29, 2003.
[31]. N. Bandara, H. Hettiarachchi, E. Jensen, T. H. Binoy, and R. Perera, "Using Kiln Dust to Improve Weak Subgrades for Pavement Construction: A Field Verification in Michigan, USA," Geotechnics, vol. 3, no. 2, pp. 179-192, 2023.
[32]. J. J. M. Moreno, A. P. Pol, A. S. Abad, and B. C. Blasco, "Using the R-MAPE index as a resistant measure of forecast accuracy," Psicothema, vol. 25, no. 4, pp. 500-506, 2013.
[33]. R. Amber. "Mean Absolute Percentage Error (MAPE): What You Need To Know." Available at: https://arize.com/blog-course/mean-absolute-percentage-error-mape-what-you-need-to-know/ (accessed 6th August, 2024).

ISSN No: -2456-2165 https://doi.org/10.38124/ijisrt/26jan986

APPENDIX

Appendix: Actual and Predicted Values of PI, CBR, UCS, C, Φ and Δ

Run	Sample Type	CKD Content	PI		CBR		UCS		C		Φ		Δ	
			Actual	Pred.	Actual	Pred.	Actual	Pred.	Actual	Pred.	Actual	Pred.	Actual	Pred.
1	KDZAR-B	10.0	1.960	1.960	25.000	24.980	0.490	0.492	11.000	11.210	33.000	33.340	1.110	1.110
2	KDM-C	10.0	2.000	2.000	21.000	20.950	0.480	0.478	19.000	19.370	29.000	28.960	0.939	0.938
3	KDZAR-B	4.0	2.450	2.450	17.000	17.200	0.190	0.173	8.000	6.620	40.000	37.700	1.170	1.180
4	KDM-A	6.0	2.560	2.570	22.000	22.400	0.880	0.849	7.000	7.650	35.000	36.080	0.922	0.945
5	KDM-D	6.0	2.380	2.370	23.000	23.000	0.710	0.659	6.000	6.480	35.000	35.760	1.090	1.110
6	KDZAR-B	8.0	2.090	2.090	21.000	21.100	0.390	0.382	11.000	10.490	34.000	34.540	1.120	1.130
7	KDM-A	10.0	2.490	2.490	27.000	27.040	1.060	1.060	10.000	10.210	33.000	32.960	0.889	0.891
8	KDZAR-B	4.0	2.450	2.450	17.000	17.200	0.190	0.173	8.000	6.620	40.000	37.700	1.170	1.180
9	KDZAR-B	0.0	2.560	2.560	16.000	16.020	0.120	0.118	4.000	5.710	39.000	39.050	1.230	1.230
10	KDZAR-A	0.0	2.390	2.390	18.000	17.980	0.260	0.260	5.000	4.370	39.000	39.340	1.690	1.700
11	KDM-D	10.0	2.220	2.220	27.000	27.000	0.970	0.965	9.000	9.040	32.000	32.010	1.010	1.010
12	KDM-B	4.0	2.440	2.430	10.000	9.920	0.290	0.276	14.000	14.290	32.000	33.350	0.888	0.868
13	KDM-D	4.0	2.360	2.370	20.000	20.000	0.510	0.561	5.000	4.460	37.000	36.960	1.200	1.180
14	KDM-D	2.0	2.350	2.350	20.000	20.000	0.660	0.635	5.000	3.170	37.000	37.150	1.220	1.230
15	KDM-D	4.0	2.360	2.370	20.000	20.000	0.510	0.561	5.000	4.460	37.000	36.960	1.200	1.180
16	KDM-A	4.0	2.540	2.530	19.000	18.600	0.740	0.771	5.000	5.620	37.000	36.970	1.000	0.977
17	KDM-B	8.0	2.490	2.490	15.000	14.960	0.500	0.493	19.000	18.150	32.000	31.570	0.811	0.801
18	KDZAR-B	0.0	2.560	2.560	16.000	16.020	0.120	0.118	4.000	5.710	39.000	39.050	1.230	1.230
19	KDM-B	0.0	2.370	2.370	9.000	8.990	0.140	0.139	16.000	13.370	33.000	33.340	0.903	0.901
20	KDZAR-B	6.0	2.370	2.370	19.000	18.800	0.230	0.247	9.000	8.650	37.000	36.690	1.150	1.140
21	KDZAR-A	2.0	2.380	2.390	16.000	16.120	0.320	0.319	7.000	4.000	38.000	37.460	1.430	1.410
22	KDZAR-A	2.0	2.380	2.390	16.000	16.120	0.320	0.319	7.000	4.000	38.000	37.460	1.430	1.410
23	KDM-A	2.0	2.500	2.510	17.000	17.200	0.700	0.685	7.000	4.330	36.000	36.850	0.997	1.010
24	KDM-B	2.0	2.390	2.390	11.000	11.040	0.220	0.227	6.000	13.000	34.000	32.660	0.829	0.839
25	KDM-A	8.0	2.590	2.580	25.000	24.800	0.920	0.935	9.000	9.490	35.000	34.040	0.977	0.966
26	KDM-D	8.0	2.340	2.340	26.000	26.000	0.890	0.915	7.000	8.320	34.000	33.400	1.050	1.050
27	KDM-C	0.0	2.180	2.180	14.000	14.050	0.120	0.122	14.000	13.870	33.000	33.100	1.070	1.070

ISSN No: -2456-2165 https://doi.org/10.38124/ijisrt/26jan986

28	KDZAR-B	6.0	2.370	2.370	19.000	18.800	0.230	0.247	9.000	8.650	37.000	36.690	1.150	1.140
29	KDM-C	4.0	2.330	2.340	15.000	15.520	0.220	0.242	16.000	14.790	35.000	32.370	1.000	1.010
30	KDZAR-A	6.0	2.440	2.460	22.000	22.240	0.410	0.408	6.000	7.310	35.000	35.440	1.500	1.450
31	KDM-D	0.0	2.290	2.290	18.000	18.000	0.540	0.545	3.000	3.540	39.000	38.720	1.440	1.440
32	KDZAR-B	2.0	2.380	2.380	18.000	17.900	0.150	0.159	5.000	5.330	36.000	37.690	1.190	1.190
33	KDZAR-A	10.0	2.080	2.080	26.000	26.020	0.510	0.510	10.000	9.870	31.000	31.050	1.340	1.340
34	KDM-A	6.0	2.560	2.570	22.000	22.400	0.880	0.849	7.000	7.650	35.000	36.080	0.922	0.945
35	KDZAR-A	8.0	2.470	2.460	25.000	24.880	0.440	0.441	8.000	9.150	33.000	32.770	1.380	1.400
36	KDM-D	10.0	2.220	2.220	27.000	27.000	0.970	0.965	9.000	9.040	32.000	32.010	1.010	1.010
37	KDZAR-B	2.0	2.380	2.380	18.000	17.900	0.150	0.159	5.000	5.330	36.000	37.690	1.190	1.190
38	KDM-D	0.0	2.290	2.290	18.000	18.000	0.540	0.545	3.000	3.540	39.000	38.720	1.440	1.440
39	KDM-A	0.0	2.530	2.530	18.000	17.960	0.590	0.593	4.000	4.710	39.000	38.100	1.000	1.000
40	KDZAR-A	6.0	2.440	2.460	22.000	22.240	0.410	0.408	6.000	7.310	35.000	35.440	1.500	1.450
41	KDM-C	6.0	2.370	2.360	18.000	17.480	0.380	0.358	17.000	16.810	30.000	31.680	0.999	0.993
42	KDM-D	6.0	2.380	2.370	23.000	23.000	0.710	0.659	6.000	6.480	35.000	35.760	1.090	1.110
43	KDM-C	2.0	2.100	2.090	17.000	16.740	0.170	0.159	12.000	13.500	31.000	32.050	1.000	1.000
44	KDM-B	6.0	2.480	2.490	12.000	12.080	0.350	0.364	19.000	16.310	33.000	33.040	0.817	0.837
45	KDM-C	0.0	2.180	2.180	14.000	14.050	0.120	0.122	14.000	13.870	33.000	33.100	1.070	1.070
46	KDM-C	8.0	2.070	2.080	20.000	20.260	0.450	0.461	19.000	18.650	30.000	29.840	0.980	0.983
47	KDM-D	2.0	2.350	2.350	20.000	20.000	0.660	0.635	5.000	3.170	37.000	37.150	1.220	1.230
48	KDZAR-A	4.0	2.420	2.400	18.000	17.760	0.370	0.372	4.000	5.290	37.000	36.950	1.400	1.440
49	KDM-B	10.0	2.220	2.220	16.000	16.010	0.580	0.581	20.000	18.870	31.000	31.050	0.803	0.805
50	KDM-B	10.0	2.220	2.220	16.000	16.010	0.580	0.581	20.000	18.870	31.000	31.050	0.803	0.805
51	KDM-C	8.0	2.070	2.080	20.000	20.260	0.450	0.461	19.000	18.650	30.000	29.840	0.980	0.983
52	KDZAR-A	0.0	2.390	2.390	18.000	17.980	0.260	0.260	5.000	4.370	39.000	39.340	1.690	1.700
53	KDM-A	10.0	2.490	2.490	27.000	27.040	1.060	1.060	10.000	10.210	33.000	32.960	0.889	0.891
54	KDM-B	6.0	2.480	2.490	12.000	12.080	0.350	0.364	19.000	16.310	33.000	33.040	0.817	0.837
55	KDM-A	4.0	2.540	2.530	19.000	18.600	0.740	0.771	5.000	5.620	37.000	36.970	1.000	0.977
56	KDM-A	8.0	2.590	2.580	25.000	24.800	0.920	0.935	9.000	9.490	35.000	34.040	0.977	0.966
57	KDM-B	4.0	2.440	2.430	10.000	9.920	0.290	0.276	14.000	14.290	32.000	33.350	0.888	0.868

ISSN No: -2456-2165 https://doi.org/10.38124/ijisrt/26jan986

58	KDM-C	6.0	2.370	2.360	18.000	17.480	0.380	0.358	17.000	16.810	30.000	31.680	0.999	0.993
59	KDZAR-B	8.0	2.090	2.090	21.000	21.100	0.390	0.382	11.000	10.490	34.000	34.540	1.120	1.130
60	KDM-B	0.0	2.370	2.370	9.000	8.990	0.140	0.139	16.000	13.370	33.000	33.340	0.903	0.901
61	KDZAR-A	4.0	2.420	2.400	18.000	17.760	0.370	0.372	4.000	5.290	37.000	36.950	1.400	1.440
62	KDM-B	8.0	2.490	2.490	15.000	14.960	0.500	0.493	19.000	18.150	32.000	31.570	0.811	0.801
63	KDM-A	0.0	2.530	2.530	18.000	17.960	0.590	0.593	4.000	4.710	39.000	38.100	1.000	1.000
64	KDM-C	10.0	2.000	2.000	21.000	20.950	0.480	0.478	19.000	19.370	29.000	28.960	0.939	0.938
65	KDZAR-A	8.0	2.470	2.460	25.000	24.880	0.440	0.441	8.000	9.150	33.000	32.770	1.380	1.400
66	KDZAR-B	10.0	1.960	1.960	25.000	24.980	0.490	0.492	11.000	11.210	33.000	33.340	1.110	1.110
67	KDM-A	2.0	2.500	2.510	17.000	17.200	0.700	0.685	7.000	4.330	36.000	36.850	0.997	1.010
68	KDZAR-A	10.0	2.080	2.080	26.000	26.020	0.510	0.510	10.000	9.870	31.000	31.050	1.340	1.340
69	KDM-B	2.0	2.390	2.390	11.000	11.040	0.220	0.227	6.000	13.000	34.000	32.660	0.829	0.839
70	KDM-D	8.0	2.340	2.340	26.000	26.000	0.890	0.915	7.000	8.320	34.000	33.400	1.050	1.050
71	KDM-C	4.0	2.330	2.340	15.000	15.520	0.220	0.242	16.000	14.790	35.000	32.370	1.000	1.010
72	KDM-C	2.0	2.100	2.090	17.000	16.740	0.170	0.159	12.000	13.500	31.000	32.050	1.000	1.000